GeoScienceWorld
Lithosphere
Volume 2022, Article ID 6518010, 11 pages
https://doi.org/10.2113/2022/6518010

Lithosphere

Research Article

Effect of Heterogeneity on the Failure of Rock with an Initial Crack under Uniaxial Compressions: A Numerical Study

Qifeng Guo,[1,2] Wei Hong,[1,2] Xun Xi,[1,2] Jiliang Pan,[1,2] and Ying Zhang[1,2]

[1]*School of Civil and Resource Engineering, University of Science and Technology Beijing, Beijing 100083, China*
[2]*Beijing Key Laboratory of Urban Underground Space Engineering, University of Science and Technology Beijing, Beijing 100083, China*

Correspondence should be addressed to Xun Xi; xixun@ustb.edu.cn

Received 12 June 2022; Accepted 30 July 2022; Published 12 August 2022

Academic Editor: Shaofeng Wang

Failure mechanisms of rock are intrinsically intertwined with heterogeneity and natural fracture. However, the effects of heterogeneity on the failure of rock with natural cracks are still far from clear. By simultaneously considering rock heterogeneity and natural fractures, this paper investigated the effects of heterogeneity on the failure of rock with a single initial crack under uniaxial compressions. The RFPA method with consideration of materials properties heterogeneity was employed, and numerical models with different crack angles were developed. The stress-strain curve, crack development, failure pattern, and AE characteristics were obtained. The numerical results were also compared with experimental results. Further, the effects of initial crack angle and heterogeneity on the strength, failure pattern, and acoustic emission (AE) characteristics were investigated by parametric studies. It has been found that, for a small homogeneity, rock failure is dominated by numerous microcracks within the crack bands that are smeared from the initial crack tips to the loading ends. Rock failure is dominated by macrocracks propagated from the initial crack tips to the loading ends for a large homogeneity. A logarithmic function is proposed to describe the relationship between the uniaxial compressive strength and the homogeneity. The AE characteristics and overall damage evolution are also significantly affected by the heterogeneity.

1. Introduction

Rock failure involves multiscale, nonlinearity, and uncertainties, which is one of the most critical engineering challenges [1–6]. Due to long-term geological activities, rock composition and structure are very complex and heterogeneous in fine scales [7–10]. For example, there are numerous microcracks, multiple minerals, interfaces between minerals, and voids in rock matrix. Moreover, natural fractures that widely exist in rock masses significantly affect the deformation and failure of rock [11]. The resulting dangerous disasters have a great impact on the safe and stable operation of the engineering rock mass [12–14]. Therefore, it is necessary to consider natural fractures and heterogeneity for understanding and predicting rock failure.

In the past decades, considerable research has been carried out to investigate the effect of natural fracture on rock failure and analyze the mechanism of fracture propagation [15–17]. The most common method is perhaps the uniaxial compressive tests of rock with initial cracks. Yang and Jing [18] carried out uniaxial compressive tests of brittle sandstone with a single initial crack and found that the uniaxial compressive strength, Young's modulus, and peak axial strain of sandstone samples with preexisting single fissure were closely related to the fissure length and fissure angle. Zhao et al. [19] investigated the cracking and stress-strain behavior of rock-like material containing two initial cracks under uniaxial compression and found local tensile strain concentration below or above the preexisting flaw tip caused wing or antiwing cracks, while the local compressive strain concentration near the flaw tip was related to the shear crack. Further, Yang et al. carried out uniaxial compressive tests of rock with more complex initial cracks (e.g., three cracks [20] and two oval cracks [21]). Qifeng et al. [22] employed the digital image correlation (DIC) technique to investigate the failure process of granite with a single crack

and found that the lowest strength occurred when the angle between loading direction and the crack was 60°. However, it is difficult to make an initial crack in rock preciously, and the experimental cost is high. Moreover, it has been found that the heterogeneity of rock has an important influence on the failure characteristics and mechanical responses of rock [23]. It is almost impossible to control the heterogeneity of rock in the experiment; thus, the experimental method is hard to be used for investigating the effect of heterogeneity on the failure with initial cracks.

With the rapid development of computer technology, numerical methods have been widely used in the study of rock failure [24–27]. Therefore, in light of the limitation of the experimental method on the failure of heterogeneous rock with initial crack, the numerical method has brought considerable advantages. Ma et al. [12] developed a one-dimensional radial three-phase flow model of water–rock–silt to investigate hydraulic characteristics of fault rock during the water–silt inrush. Wang et al. [11] employed particle flow code (PFC2D) to simulate the failure of rock with hole, single crack, and multiple cracks. They found most cracks appeared after peak strength, and different shapes, the number of defects, and the relative defect positions significantly affected crack initiation, propagation, and coalescence. Xi et al. [28] modeled the fracture propagation process of rock with a single crack by the extended finite element method (XFEM) and found the crack propagation speed was affected by the initial crack angle. Liu et al. [29] considered the heterogeneity of rock as particle sizes in PFC and modeled the failure of rock with different heterogeneity. Tang et al. [30] developed a rock failure process analysis method (RFPA) to model rock failure considering rock heterogeneity as Weibull distribution. Li et al. [31] employed RFPA to simulate borehole failure under different stress conditions. Kong et al. [32] implemented Weibull distribution of rock properties into FLAC3D and modeled tunnel stability in a coal mine. Zhang et al. [33] modeled rock fracture by Voronoi cells and combined finite and discrete element method (FDEM). Mondal et al. [34] developed a finite element method by Python and considered the heterogeneity of materials properties as Weibull distribution for modeling rock failure affected by heterogeneity. However, the effects of rock heterogeneity on the failure of rock with initial crack are rarely to be investigated. The failure mechanisms, including the strength, failure pattern, and acoustic emissions (AE) characteristics of heterogeneous rock with initial crack, are still far from clear.

This paper attempts to investigate the effect of heterogeneity on the failure of rock with a single crack under uniaxial compressions. The RFPA method with consideration of material property heterogeneity is employed, and rock with different crack angles is modeled. The stress-strain curve, crack development, failure pattern, and AE characteristics are obtained. The numerical results are compared with experimental results. Further, the effects of initial crack angle and heterogeneity on the strength, failure pattern, and AE characteristics are investigated by parametric studies. Finally, the overall damage evolution of rock affected by heterogeneity is discussed.

2. Methodology

2.1. Basic Description of Numerical Method. RFPA developed by Tang has been widely used to model rock failure under complex loading conditions [35–37]. In this study, RFPA2D was employed to simulate the uniaxial compressive tests of rock with an initial crack. A basic principle for the numerical method is considering heterogeneous distributions of rock mechanical parameters. The mechanical parameters including strength and elastic modulus can be described by Weibull distribution function [38], which is expressed as follows:

$$\varphi(\alpha) = \frac{m}{\alpha_0} \cdot \left(\frac{\alpha}{\alpha_0}\right)^{m-1} \cdot \exp\left[-\left(\frac{\alpha}{\alpha_0}\right)^{m}\right], \tag{1}$$

where $\varphi(\alpha)$ is the probability density function of the mechanical parameter α, α_0 is the average value for the mechanical parameter, and m is the shape of the distribution which defines the homogeneity of rock.

The cumulative distribution function of the mechanical parameter can thus be expressed as follows:

$$P(\alpha) = 1 - \exp\left[-\left(\frac{\alpha}{\alpha_0}\right)^{m}\right], \tag{2}$$

where $P(\alpha)$ is the cumulative distribution function.

The larger the homogeneity parameter m is, the more homogeneous the rock is [39]. Taking $\alpha_0 = 200$ as an example, Figure 1 illustrates the probability density function and cumulative distribution function of rock for different values of m. It can be seen that, the larger the m is, the mechanical parameter is more focused on its average value. The smaller the m is, the larger the randomness of the parameter is and the more heterogeneity the material is. Therefore, the assumption of Weilbull failure theory in RFPA provides a flexible method for investigating materials heterogeneity on rock failure.

The damage law is based on the linear elastic damage theory [40]:

$$\sigma = E\varepsilon = E_0\varepsilon(1 - D), \tag{3}$$

where σ is the stress, E is the elastic modulus with damage, E_0 is the initial elastic modulus, ε is the strain, and D is the damage value.

The damage evolution by tensile strain is expressed as follows [41]:

$$D = \begin{cases} 0 & \varepsilon < \varepsilon_{t0}, \\ 1 - \dfrac{f_{\mathrm{tr}}}{E_0\varepsilon} & \varepsilon_{t0} \le \varepsilon \le \varepsilon_{\mathrm{tu}}, \\ 1 & \varepsilon > \varepsilon_{\mathrm{tu}}, \end{cases} \tag{4}$$

where ε_{t0} is the critical strain to damage initiation, f_{tr} is the residual strength, and $\varepsilon_{\mathrm{tu}}$ is the critical failure strain to complete failure.

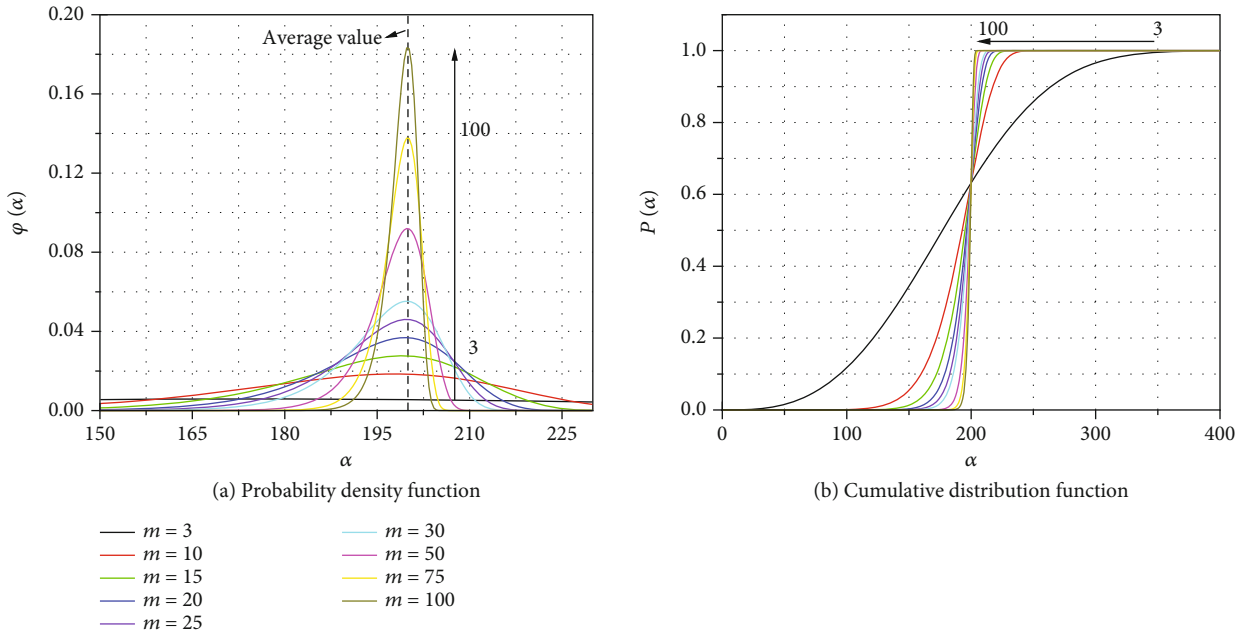

FIGURE 1: Probability density function and cumulative distribution function of rock parameter for different values of homogeneity.

The damage evolution by compressive strain can be expressed as follows [41]:

$$D = \begin{cases} 0 & \varepsilon < \varepsilon_{c0}, \\ 1 - \dfrac{\sigma_{rc}}{E_0 \varepsilon} & \varepsilon \geq \varepsilon_{c0}, \end{cases} \tag{5}$$

where ε_{c0} is the critical compressive strain to damage initiation, and σ_{rc} is the residual uniaxial compressive strength.

The overall damage is the maximum value between compressive and tensile strains. Further, the overall damage of the numerical model can be expressed as the ratio of failed elements number to total elements number N, i.e.,

$$D_m = \frac{N_{AE}}{N}, \tag{6}$$

where D_m is the overall damage of the numerical model, and N_{AE} is the number of failed elements which are also recorded as the acoustic emission events. The energy release during element failure can be calculated as follows [42]:

$$W_i = \frac{1}{2E}\left(\sigma_1^2 + \sigma_3^2 - 2\nu\sigma_1\sigma_3\right)V, \tag{7}$$

where W_i is the energy release amount for element number i; σ_1 and σ_3 are the maximum and minimum principal stress, respectively. ν is Poisson's ratio; V is the element volume.

2.2. Numerical Model. A worked example for rock with dimensions of 50 mm × 100 mm is developed. The initial crack has a length of 20 mm. The incline angle between the crack and loading direction is 45°. Figure 2 shows the dimensions of the model and the numerical model in RFPA. There are 20,000 square elements in total with the size of 0.5 mm. The color represents the value of the mechanical parameter. The homogeneity parameter m is 3.0 in the model. Figure 2(c) shows the heterogeneity for the elements in the model. The loading is controlled by a displacement rate of 0.005 mm per step. To investigate the effects of heterogeneity on the failure of rock, the homogeneity m is set as 1, 1.5, 3.0, 5.0, 10, 15, 20, 30, 50, and 70, respectively. All the basic mechanical parameters are given in Table 1.

3. Results and Verification

3.1. Failure Process of Rock. Typical stress, strain, and crack developments are first discussed by a worked example for $\beta = 45°$ and $m = 3$. Figure 3 illustrates the stress-strain curve and cracks development process. It can be found that, with the strain increasing, the stress first almost linearly increases then suddenly drops after the peak stress. The compressive strength is 37.69 MPa. The difference between the simulated strength of the specimen and the mean strength of elements is caused by rock heterogeneity and the initial crack. Two macrocracks propagate from the initial crack tips due to stress concentrations at the stress about half of the peak stress (point B). And the macrocracks propagate to the direction of the axial load from point B to point C. During about 84% of peak stress to peak stress, secondary antiwing cracks appear from the initial crack tip to the loading direction. Therefore, the initial crack dominates the crack location and patterns of rock.

3.2. Stress-Strain Curves and Failure Patterns for Rock with Different Homogeneity. Figure 4 illustrates the stress-strain

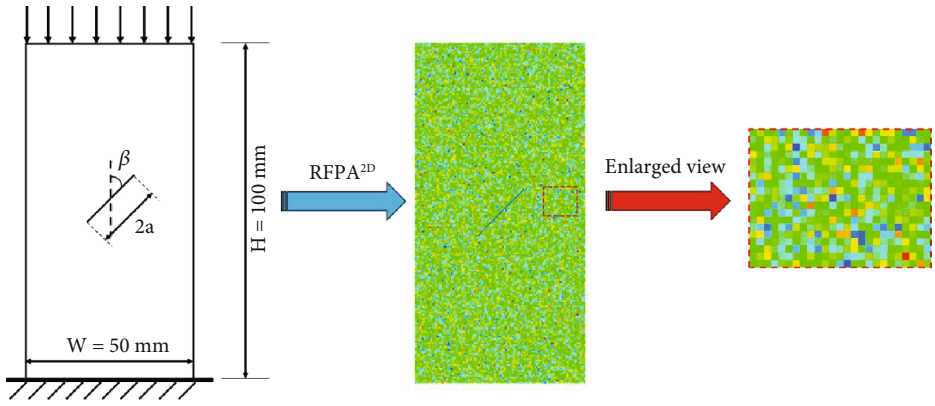

(a) Dimensions (b) Numerical model (c) Heterogeneity

Figure 2: Numerical model for the crack angle 45°.

Table 1: The basic mechanical parameters in the models.

Parameter	Value
Homogeneity	1, 1.5, 3.0, 5.0, 10, 15, 20, 30, 50, 70
Young's modulus (GPa)	17.525
Poisson's ratio	0.3
Frictional angle (°)	42.7
Mean strength (MPa)	240

curves for rock with the crack angle 45° and homogeneity 1-30. It can be found that, for the homogeneity 1 and 1.5, with the increasing of strain, the axial stress first linearly increases, and then nonlinearly increases until peak stress. However, for the homogeneity 3-30, the axial stress almost linearly increases until the peak stress with the strain increasing. After the peak stress, there is a sudden drop of stress, which indicates the brittle failure of rock. Further, the critical strain to peak stress is similar for a small homogeneity in the range of 1-3. But for the homogeneity larger than 3, the larger the homogeneity is, the larger the critical strain to peak stress is. Figure 5 shows the failure patterns for rock with the crack angle 45° and homogeneity 1-30. It can be seen that the failure patterns are significantly changed by the homogeneity. For the homogeneity 1-5, there are not only dominated macrocracks but only numerous microcracks in the failed rock. The dominated macrocracks are antiwing cracks, secondary cracks, and wing cracks for rock with the homogeneity 1-5. However, for the homogeneity larger than 5, there are only two wing cracks which cause rock failure. The dominated cracks are all connected by the initial crack. Therefore, the failure pattern of rock is controlled by the initial crack and significantly affected by the homogeneity. For a small homogeneity, the failure of rock is dominated by numerous microcracks within the crack bands that are smeared from the initial crack tips to the loading ends. For a large homogeneity, the failure of rock is dominated by macrocracks propagated from the initial crack tip to the loading direction.

3.3. Verification. To verify the numerical method, the failure patterns and strengths for rock with different crack angles from numerical simulations are compared with those from previous experiments conducted by the authors [22]. Granite specimens with different crack angles were prepared for uniaxial compressive tests in [22]. The specimens were cubes thus can be modeled through a two-dimensional plan strain model. The dimensions of the model were the same as those in experiments, i.e., 50 mm × 100 mm. Granite is a typical heterogeneous rock which is determined as homogeneity 10 by trial and error. The crack angles were 0°, 30°, 45°, 60°, and 90°. The parameters are given in Table 1, and the homogeneity is 10. Figure 6 shows the uniaxial compressive strengths as a function of crack angle from experiments and numerical simulations. It can be seen that the predicted strengths for different crack angles from numerical simulations have a good agreement with those from experiments. For the crack angle varying from 0 to 90°, the compressive strength first decreases then increases. The lowest strength occurs for the specimen with the crack angle 60°. This is because the crack initiation at the crack tip for crack angle 60° is more prone to occur. The uniaxial compressive strength for specimen with initial crack angle 0 is the highest. Figure 7 shows the failure patterns for different crack angles from numerical and experimental results. It can be found that the crack patterns from numerical results are generally consistent with experimental results. For the specimen with initial crack angle 0, a straight crack initials from the initial crack tip and propagates to the loading end. This is because the initial crack would be opened under axial compressive stress. The crack patterns for the initial crack angle 30-60° are relatively simple. However, the crack patterns for the initial crack angle 90° are relatively complex because the initial crack would be closed under axial compressive stress. The complex failure patterns for the initial crack angle 90° lead to a significant difference of strength between numerical and experimental results. Through comprehensive comparisons of strengths and failure patterns for different angles, it can be concluded that the employed numerical method is reliable.

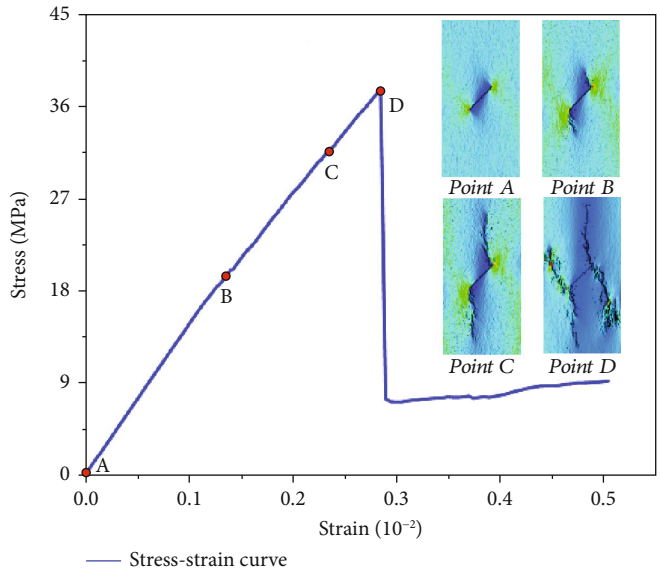

Figure 3: Stress-strain curve and failure process for $m = 3$.

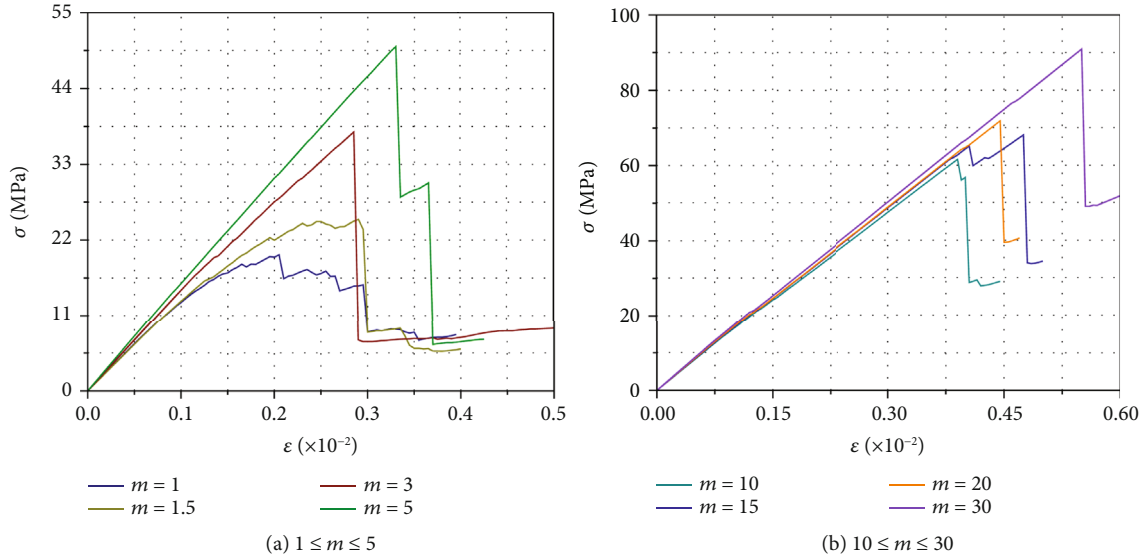

(a) $1 \le m \le 5$ (b) $10 \le m \le 30$

Figure 4: Stress-strain curves for rock models with different values of homogeneity.

4. Analysis and Discussion

4.1. Effects of Heterogeneity on Rock Strength. To further investigate the effects of heterogeneity on rock strength, the uniaxial compressive strengths of rock models with the initial crack angle 45° are plotted in Figure 8. It can be found that, with the increasing of homogeneity, the uniaxial compressive strength firstly increases then keeps almost constant after the homogeneity larger than 30. The uniaxial compressive strength for m larger than 30 is about 4.58 times of that for $m = 1$. Thus, the heterogeneity has a strong influence on the strength of rock with the initial crack. Further, a logarithmic function is proposed to describe the relationship between the uniaxial compressive strength and the homogeneity. The function is obtained through nonlinear fitting as follows:

$$\sigma_c = 19.63359 + 17.83294 \ln^{(m-0.03876)} (m \le 30) \left(R^2 = 0.9785\right), \tag{8}$$

where σ_c is the uniaxial compressive strength.

It can be seen from Figure 8 that, for m smaller than 30, the logarithmic function can well describe the relationship between the uniaxial compressive strength and the homogeneity.

4.2. Effects of Heterogeneity on AE Characteristics. Acoustic emission (AE) is the phenomenon of elastic waves in solids that occurs when a material undergoes irreversible changes

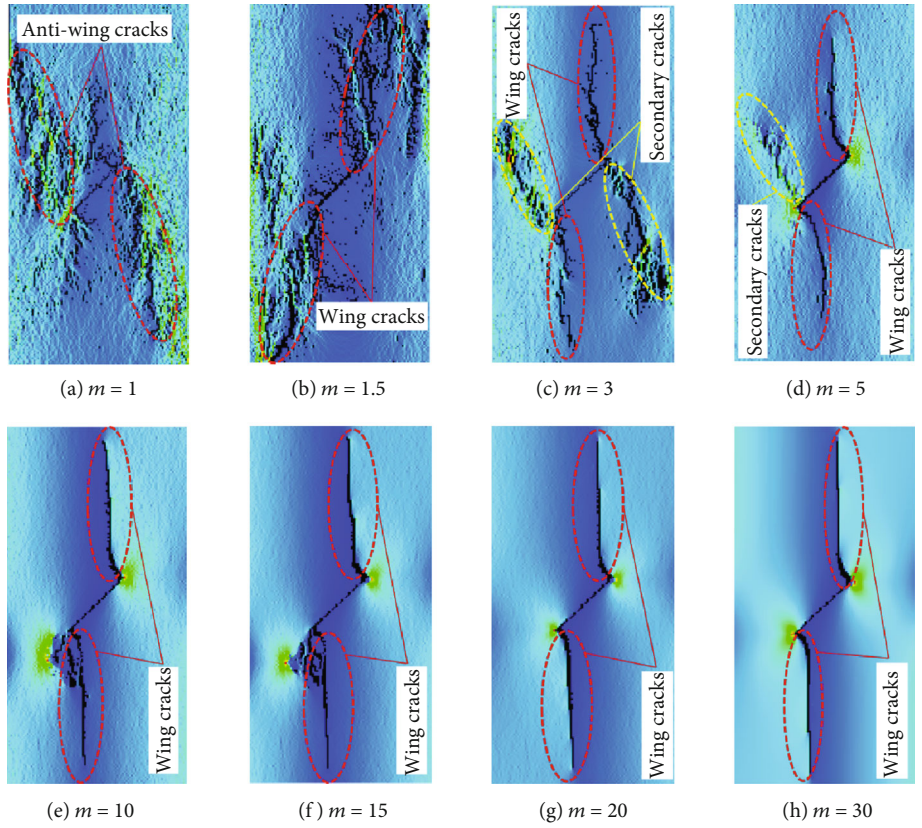

(a) $m = 1$ (b) $m = 1.5$ (c) $m = 3$ (d) $m = 5$

(e) $m = 10$ (f) $m = 15$ (g) $m = 20$ (h) $m = 30$

Figure 5: Failure patterns for rock models with different values of homogeneity.

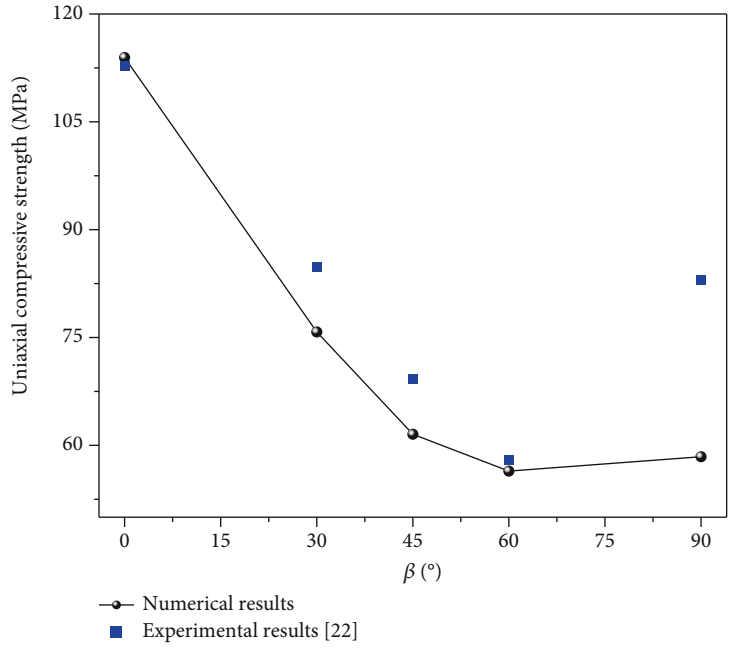

Figure 6: Comparisons of uniaxial compressive strengths between numerical and experimental results [22].

in its internal structure. The generation, nucleation, and propagation of cracks in rock during the loading process will emit energy outward as elastic waves [43]. The AE characteristics are crucial for understanding rock failure [44, 45]. In RFPA, the AE counts are defined as the number of failed elements during a step increment, and the accumulated AE counts is the total number of failed elements. Figure 9 illustrates the AE counts and accumulated AE counts during the

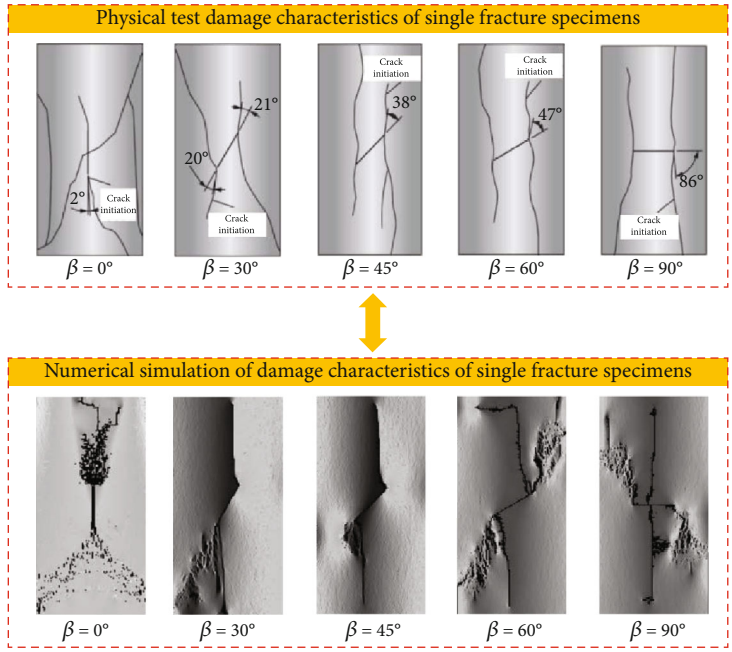

Figure 7: Comparisons of failure patterns between numerical and experimental results [22].

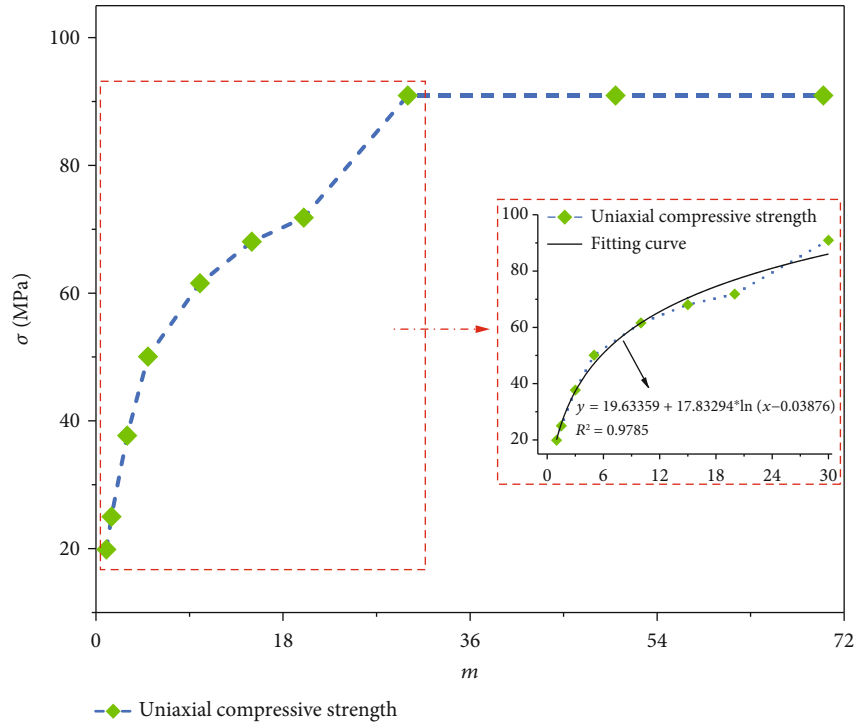

Figure 8: Effect of homogeneity on uniaxial compressive strength of rock with initial crack.

uniaxial compressive loading for rock with the crack angle 45° for different values of homogeneity. According to the AE counts in Figure 9, the deformation and failure processes of rock with the initial crack can be divided into four stages: (1) no AE events (before point A), (2) AE growth (AB), (3) AE quiet (BC), and (4) AE burst (CD). During the initial loading stage, the stress is too low to fracture rock thus there is no AE events. With the stress increasing, the concentrated stress around the initial crack tip reaches the failure stress, and AE events start to accumulate. Further, during the AE quiet stage, there is no element failure because most elements with weak properties have failed. When the stress continues to increase, AE burst occurs due to the stress is over most elements in the crack bands. After the AE burst, the stress of rock is the postpeak stage. The homogeneity has significant effects on the duration of AE stages. For a

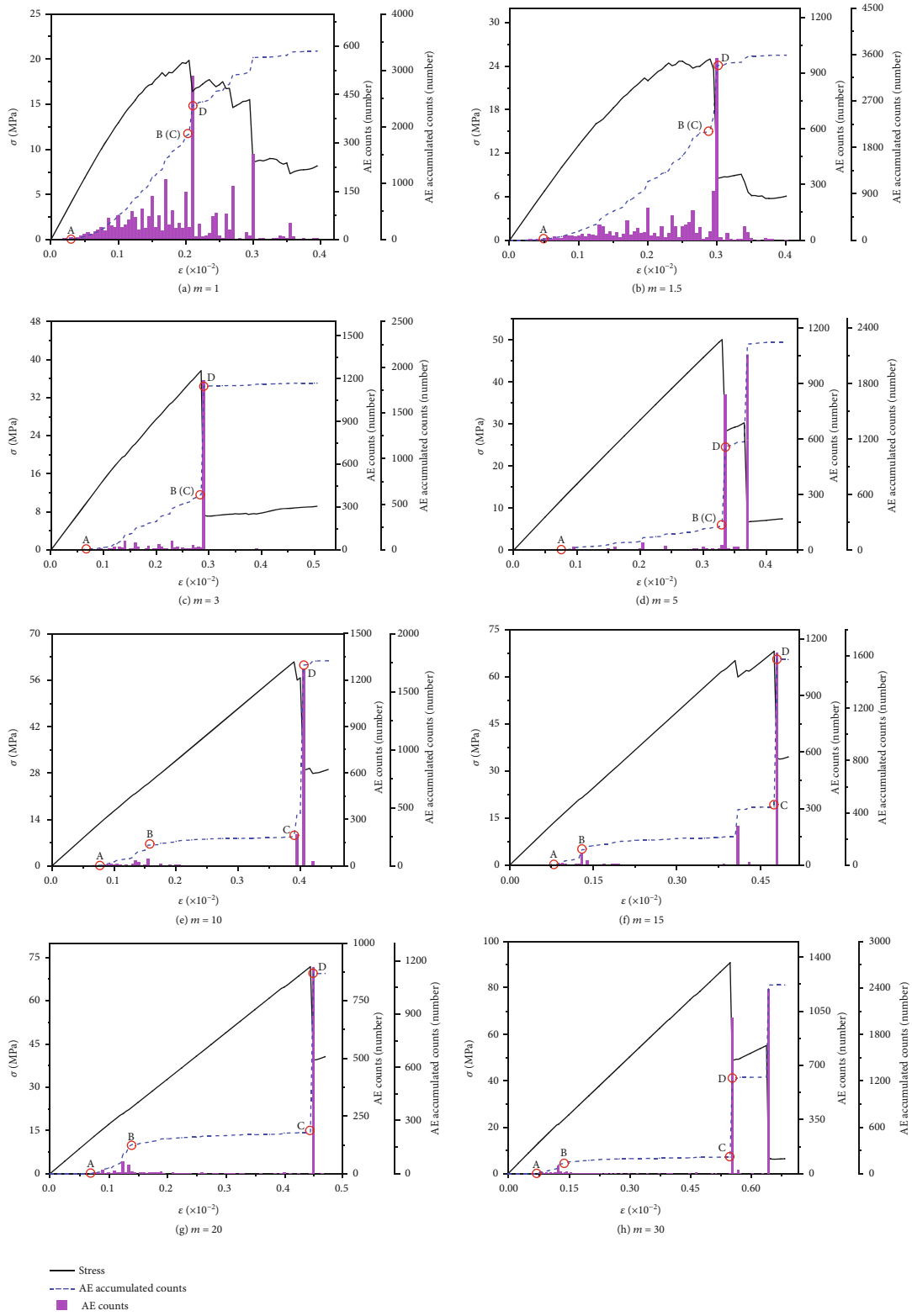

Figure 9: Effect of homogeneity on the AE characteristics.

small homogeneity ($1 \le m \le 5$), the AE quiet almost disappears because the high heterogeneity causes random failure of different elements. For a large homogeneity ($10 \le m \le 30$), the AE quiet stage lasts a long period. This is because most elements with weak properties in the crack band has been failed, and more energy is required to fail elements with

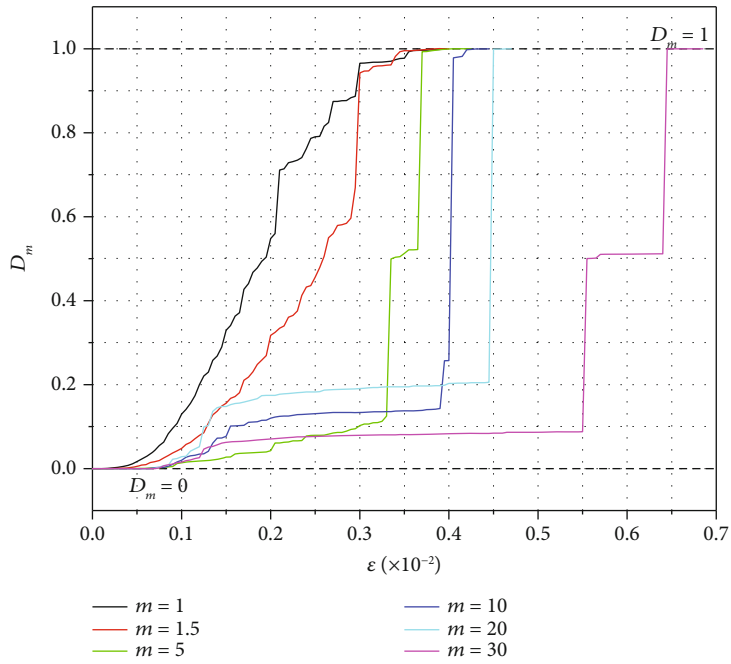

Figure 10: Effect of homogeneity on the overall damage evolution.

homogeneous strong properties. The larger the homogeneity is, the AE counts are more concentrated at a certain strain range, and the failure of rock is more brittle.

4.3. Effects of Heterogeneity on Overall Damage Evolution. Figure 10 illustrates the overall damage evolution of rock as a function of strain. The overall damage value is normalized as 0-1 for comparison. It can be seen that the overall damage values for rock with different homogeneities are about 0 before the strain 0.0005. With the strain increasing, the overall damage gradually increases until 1. Moreover, the smaller the homogeneity is, the overall damage starts to increase earlier but the increased slope is smaller. The larger the homogeneity is, the increase of overall damage is later but faster. Further, there is a flat stage of overall damage curve for homogeneity 5-30, which represents the AE quiet stage. Therefore, the homogeneity significantly affects the overall damage of rock with initial crack. The failure of rock with initial crack and high homogeneity is staged.

5. Conclusions

This paper investigated the failure of rock with an initial crack under uniaxial compressions by a numerical method considering the heterogeneity of rock. The effects of homogeneity and crack angle on rock failure were discussed by parametric studies. The numerical results were compared with previous experimental results. The AE characteristics and overall damage evolution were investigated for different homogeneity of rock. Some conclusions can be drawn as follows:

(1) The homogeneity significantly affects the failure of rock with an initial crack. For a small homogeneity, the failure of rock is dominated by numerous microcracks within the crack bands that are smeared from the initial crack tips to the loading ends. For a large homogeneity, the failure of rock is dominated by macrocracks propagated from the initial crack tips to the loading ends

(2) With the increasing of homogeneity, the uniaxial compressive strength firstly increases then keeps almost constant after the homogeneity larger than 30. The uniaxial compressive strength for m larger than 30 is about 4.58 times of that for $m = 1$. A logarithmic function can be used to describe the relationship between the uniaxial compressive strength and the homogeneity

(3) The prepeak deformation and failure processes of rock with the initial crack can be divided into four stages: no AE events, AE growth, AE quiet, and AE burst. For a small homogeneity ($1 \le m \le 5$), the AE quiet almost disappears because the high heterogeneity causes random failure of different elements. For a large homogeneity ($10 \le m \le 30$), the AE quiet stage lasts a long period

(4) The smaller the homogeneity is, the overall damage starts to increase earlier but the increased slope is smaller. The larger the homogeneity is, the increase of overall damage is later but faster

Data Availability

The data supporting these study's findings are available from the authors upon reasonable request.

Conflicts of Interest

The authors declare no competing interests.

Acknowledgments

This work is supported by the National Key Research and Development Program of China (2021YFC3001301) and the Fundamental Research Funds for the Central Universities, USTB (FRF-IDRY-20-032).

References

[1] J. Pan, M. F. Cai, P. Li, and Q. F. Guo, "A damage constitutive model of rock-like materials containing a single crack under the action of chemical corrosion and uniaxial compression," *Journal of Central South University*, vol. 29, no. 2, pp. 486–498, 2022.

[2] J. Pan, X. Wu, Q. Guo, X. Xi, and M. Cai, "Uniaxial experimental study of the deformation behavior and energy evolution of conjugate jointed rock based on AE and DIC methods," *Advances in Civil Engineering*, vol. 2020, 16 pages, 2020.

[3] Q. Guo, X. Xi, S. Yang, and M. Cai, "Technology strategies to achieve carbon peak and carbon neutrality for China's metal mines," *International Journal of Minerals, Metallurgy and Materials*, vol. 29, no. 4, pp. 626–634, 2022.

[4] M. Jiao, C.'. Tang, G. Zhang, Y. Shi, and W. Hou, "A numerical test on influence of mesoscopic heterogeneity on macroscopic behavior of rock failure and seismic sequence types," *Chinese Journal of Geophysics*, vol. 46, no. 5, pp. 943–953, 2003.

[5] Q. Liu and P. Deng, "Numerical study of rock fragmentation process and acoustic emission by FDEM based on heterogeneous model," *Mathematical Problems in Engineering*, vol. 2020, Article ID 2109584, 13 pages, 2020.

[6] L. Zhang, Y. Cong, F. Meng, Z. Wang, P. Zhang, and S. Gao, "Energy evolution analysis and failure criteria for rock under different stress paths," *Acta Geotechnica*, vol. 16, no. 2, pp. 569–580, 2021.

[7] D. Shirole, G. Walton, and A. Hedayat, "Experimental investigation of multi-scale strain-field heterogeneity in rocks," *International Journal of Rock Mechanics and Mining Sciences*, vol. 127, p. 104212, 2020.

[8] S. Jiang, M. Sharafisafa, and L. Shen, "Using artificial neural networks to predict influences of heterogeneity on rock strength at different strain rates," *Materials*, vol. 14, no. 11, p. 3042, 2021.

[9] H. Y. Liu, M. Roquete, S. Q. Kou, and P. A. Lindqvist, "Characterization of rock heterogeneity and numerical verification," *Engineering Geology*, vol. 72, no. 1-2, pp. 89–119, 2004.

[10] K. Feng and X. Zhou, "Peridynamic simulation of the mechanical responses and fracturing behaviors of granite subjected to uniaxial compression based on CT heterogeneous data," *Engineering with Computers*, pp. 1–23, 2022.

[11] S. Wang, Y. Jing, Z. Pi, S. Wang, Z. Zhou, and G. Sheng, "Strength and failure properties of preflawed granite under coupled biaxial loading and unloading conditions," *Lithosphere*, vol. 2021, no. Special 7, 2022.

[12] D. Ma, H. Duan, J. Zhang, X. Liu, and Z. Li, "Numerical Simulation of Water-silt Inrush Hazard of Fault Rock: A Three-Phase Flow Model," *Rock Mechanics and Rock Engineering*, vol. 55, pp. 5163–5182, 2022.

[13] D. Ma, H. Duan, and J. Zhang, "Solid grain migration on hydraulic properties of fault rocks in underground mining tunnel: radial seepage experiments and verification of permeability prediction," *Tunnelling and Underground Space Technology*, vol. 126, p. 104525, 2022.

[14] C. Li, D. Guo, Y. Zhang, and C. An, "Compound-mode crack propagation law of PMMA semicircular-arch roadway specimens under impact loading," *International Journal of Coal Science & Technology*, vol. 8, no. 6, pp. 1302–1315, 2021.

[15] D. Ma, H. Duan, Q. Zhang et al., "A numerical gas fracturing model of coupled thermal, flowing and mechanical effects," *CMC-Computers Materials & Continua*, vol. 65, no. 3, pp. 2123–2141, 2020.

[16] Y. Wang, X. Zhou, and M. Kou, "Three-dimensional numerical study on the failure characteristics of intermittent fissures under compressive-shear loads," *Acta Geotechnica*, vol. 14, no. 4, pp. 1161–1193, 2019.

[17] L. Dou, K. Yang, and X. Chi, "Fracture behavior and acoustic emission characteristics of sandstone samples with inclined precracks," *International Journal of Coal Science & Technology*, vol. 8, no. 1, pp. 77–87, 2021.

[18] S. Yang and H. Jing, "Strength failure and crack coalescence behavior of brittle sandstone samples containing a single fissure under uniaxial compression," *International Journal of Fracture*, vol. 168, no. 2, pp. 227–250, 2011.

[19] Y. Zhao, L. Zhang, W. Wang, C. Pu, W. Wan, and J. Tang, "Cracking and stress–strain behavior of rock-like material containing two flaws under uniaxial compression," *Rock Mechanics and Rock Engineering*, vol. 49, no. 7, pp. 2665–2687, 2016.

[20] S. Q. Yang, D. S. Yang, H. W. Jing, Y. H. Li, and S. Y. Wang, "An experimental study of the fracture coalescence behaviour of brittle sandstone specimens containing three fissures," *Rock Mechanics and Rock Engineering*, vol. 45, no. 4, pp. 563–582, 2012.

[21] S. Yang, Y. H. Huang, W. L. Tian, and J. B. Zhu, "An experimental investigation on strength, deformation and crack evolution behavior of sandstone containing two oval flaws under uniaxial compression," *Engineering Geology*, vol. 217, pp. 35–48, 2017.

[22] Q. F. Guo, X. Wu, M. F. Cai, F. Ren, and J. Pan, "Crack initiation mechanism of pre-existing cracked granite," *Journal of China Coal Society*, vol. 44, no. S02, p. 8, 2019.

[23] X. Pan, W. Guo, S. Wu, and J. Chu, "An experimental approach for determination of the Weibull homogeneity index of rock or rock-like materials," *Acta Geotechnica*, vol. 15, no. 2, pp. 375–391, 2020.

[24] X. Feng, Z. Wang, Y. Zhou, C. Yang, P. Z. Pan, and R. Kong, "Modelling three-dimensional stress-dependent failure of hard rocks," *Acta Geotechnica*, vol. 16, no. 6, pp. 1647–1677, 2021.

[25] G. Gao, M. A. Meguid, and L. E. Chouinard, "On the role of pre-existing discontinuities on the micromechanical behavior of confined rock samples: a numerical study," *Acta Geotechnica*, vol. 15, no. 12, pp. 3483–3510, 2020.

[26] F. Dai, Q. Zhang, Y. Liu, H. Du, and Z. Yan, "Experimental evaluation of sandstone under cyclic coupled compression-shear loading: fatigue mechanical response and failure behavior," *Acta Geotechnica*, vol. 17, pp. 3315–3336, 2022.

[27] Y. Chen, J. Zuo, D. Liu, Y. Li, and Z. Wang, "Experimental and numerical study of coal-rock bimaterial composite bodies

under triaxial compression," *International Journal of Coal Science & Technology*, vol. 8, no. 5, pp. 908–924, 2021.

[28] X. Xi, X. Wu, Q. Guo, and M. Cai, "Experimental investigation and numerical simulation on the crack initiation and propagation of rock with pre-existing cracks," *IEEE Access*, vol. 8, pp. 129636–129644, 2020.

[29] G. Liu, M. Cai, and M. Huang, "Mechanical properties of brittle rock governed by micro-geometric heterogeneity," *Computers & Geotechnics*, vol. 104, pp. 358–372, 2018.

[30] C. Tang, H. Liu, P. K. K. Lee, Y. Tsui, and L. G. Tham, "Numerical studies of the influence of microstructure on rock failure in uniaxial compression – Part I: effect of heterogeneity," *International Journal of Rock Mechanics & Mining Sciences*, vol. 37, no. 4, pp. 555–569, 2000.

[31] Y. Li, Y. Qu, Q. He, and C. Tang, "Mesoscale numerical study on the evolution of borehole breakout in heterogeneous rocks," *International Journal for Numerical and Analytical Methods in Geomechanics*, vol. 44, no. 8, pp. 1219–1236, 2020.

[32] P. Kong, L. Jiang, J. Shu, A. Sainoki, and Q. Wang, "Effect of fracture heterogeneity on rock mass stability in a highly heterogeneous underground roadway," *Rock Mechanics and Rock Engineering*, vol. 52, no. 11, pp. 4547–4564, 2019.

[33] S. Zhang, S. Qiu, P. Kou, S. Li, P. Li, and S. Yan, "Investigation of damage evolution in heterogeneous rock based on the grain-based finite-discrete element model," *Materials*, vol. 14, no. 14, p. 3969, 2021.

[34] S. Mondal, L. M. Olsen-Kettle, and L. Gross, "Sensitivity of the damage response and fracture path to material heterogeneity present in a sandstone specimen containing a pre-existing 3-D surface flaw under uniaxial loading," *Computers and Geotechnics*, vol. 126, p. 103728, 2020.

[35] T. Li, Tang, Rutqvist et al., "The influence of an interlayer on dual hydraulic fractures propagation," *Energies*, vol. 13, no. 3, p. 555, 2020.

[36] T. Li, J. Rutqvist, and M. Hu, "TOUGH-RFPA: coupled thermal-hydraulic-mechanical rock failure process analysis with application to deep geothermal wells," *International Journal of Rock Mechanics and Mining Sciences*, vol. 142, article 104726, 2021.

[37] X. Liu, Z. Liang, S. Meng, C. Tang, and J. Tao, "Numerical simulation study of brittle rock materials from micro to macro scales using digital image processing and parallel computing," *Applied Sciences*, vol. 12, no. 8, p. 3864, 2022.

[38] W. Weibull, "A statistical distribution function of wide applicability," *Journal of Applied Mechanics*, vol. 18, no. 3, pp. 293–297, 1951.

[39] C. Tang, "Numerical simulation of progressive rock failure and associated seismicity," *International Journal of Rock Mechanics and Mining Sciences*, vol. 34, no. 2, pp. 249–261, 1997.

[40] B. Fu, Y. Li, C.'. Tang, and Z. Lin, "Failure of rock slope with heterogeneous locked patches: insights from numerical modelling," *Applied Sciences*, vol. 11, no. 18, p. 8585, 2021.

[41] S. Y. Wang, S. W. Sloan, D. C. Sheng, and C. A. Tang, "3D numerical analysis of crack propagation of heterogeneous notched rock under uniaxial tension," *Tectonophysics*, vol. 677-678, pp. 45–67, 2016.

[42] C. A. Tang, L. G. Tham, S. H. Wang, H. Liu, and W. H. Li, "A numerical study of the influence of heterogeneity on the strength characterization of rock under uniaxial tension," *Mechanics of Materials*, vol. 39, no. 4, pp. 326–339, 2007.

[43] X. Liu, Z. Liu, X. Li, F. Gong, and K. du, "Experimental study on the effect of strain rate on rock acoustic emission characteristics," *International Journal of Rock Mechanics and Mining Sciences*, vol. 133, p. 104420, 2020.

[44] S. Li and G. Li, "Effect of heterogeneity on mechanical and acoustic emission characteristics of rock specimen," *Journal of Central South University of Technology*, vol. 17, no. 5, pp. 1119–1124, 2010.

[45] A. Li, G. J. Shao, J. B. Su, Y. Sun, T. T. Yu, and H. G. Shi, "Influence of heterogeneity on mechanical and acoustic emission behaviours of stratified rock specimens," *European Journal of Environmental and Civil Engineering*, vol. 22, no. sup1, pp. s381–s414, 2018.